Hindawi
Shock and Vibration
Volume 2020, Article ID 8810089, 12 pages
https://doi.org/10.1155/2020/8810089

Research Article

Analysis of Cumulative Damage for Shared Rock in a Neighborhood Tunnel under Cyclic Blasting Loading Using the Ultrasonic Test

Feng Cao,[1] Sheng Zhang ,[2,3] and Tonghua Ling[4]

[1]*Hunan Provincial Communications Planning, Survey and Design Institute Company Limited, Changsha 410200, China*
[2]*School of Civil Engineering, Hunan City University, Yiyang 413000, China*
[3]*Department of Mechanical Engineering, University of Houston, Houston, TX 77204, USA*
[4]*School of Civil Engineering, Changsha University of Science & Technology, Changsha 410114, China*

Correspondence should be addressed to Sheng Zhang; zhangsheng0403311@163.com

Received 28 August 2020; Accepted 7 September 2020; Published 21 September 2020

Academic Editor: Guangchao Zhang

In blasting excavation of neighborhood tunnels, damage accumulation process in surrounding rock is inevitable. To explore the influence of damage accumulation of rock mass under multiple blasting loads, we analyzed the vibration damage accumulation process of ultrasonic wave velocity of rock mass in shared rock of Liuyuetian neighborhood tunnel through ultrasonic test. Moreover, the effects of cyclic blasting loads on damage to the shared rock in the neighborhood tunnel were discussed and reported. The results demonstrate that the damage accumulation to the shared rock in the neighborhood tunnel is generated after multicycle progressive blasting operations. Influenced by cyclic blasting loads during the posterior excavating tunnel, the damage range of shared rock at the anterior excavating tunnel is 1.2 to 1.4 m, and the damage range of shared rock at the posterior excavating tunnel is 2.2 to 2.4 m. The damage range of shared rock in the posterior excavating tunnel is about 1.71 to 1.83 times that in the anterior excavating tunnel. Under blasting load, the stress concentration zone of shared rock is close to the blasting excavating face and is mainly within 2 m along the longitudinal axis of the tunnel. With continuous advancement of the blasting excavating face, the stress concentration zone moves forward continuously, and a striped stress concentration zone, which is approximately 2 m deep, is formed gradually. Thus, a method was proposed to determine the damage range of shared rock in the neighborhood tunnel during blasting excavation, as well as the variation law of damage. The experiences and conclusions presented can be used as references in the design and construction of similar engineering projects in the future.

1. Introduction

Drilling and blasting method has been widely used in mining, hydropower, transportation, and other industries due to its advantages such as low cost, simple construction technology, and possibility to deal with various shapes and sizes of openings [1–5]. When the drilling and blasting method is used to excavate the rock mass in the neighborhood tunnel, the blasting vibration may influence the surrounding rock, support system, and lining structure of the tunnel significantly [6–10]. How to ensure the stability of the lining structure, support system, and shared rock of the tunnel, and relieving adverse effects of blasting vibration is the challenge in tunnel engineering construction. As the major load-carrying structure of the neighborhood tunnel, the shared rock is not only an essential support system but also the weak position of the tunnel structure [11–14]. For the rock mass of the neighborhood tunnel, the changing clear spacing and complex stress structure may influence the stability of the surrounding rock [15–19]. In particular, the rock masses of the tunnel are often excavated by cyclic progressive blasting method. Multiple disturbances to the same position in remaining rock and even in shared rock can easily cause propagation of microcracks, thereby resulting in continuous deterioration of mechanical properties, continuous reduction of material strength, and gradual

deterioration of stability [20–22]. This condition causes instability of the tunnel support system. Owing to the unique construction technology, complex structural form, and stress state, as well as frequent blasting vibration, the vibration effects and damage features of surrounding rock are highly complicated [23, 24]. Therefore, studying the damage mechanism and evolution process of shared rock in the neighborhood tunnel is an important task.

Over the years, abundant studies on rock damage caused by blasting have been reported, mostly based on field investigations and laboratory experiments [25–28]. The damage of rock mass in underground mining and tunneling has been described in terms of blast-induced rock mass damage, rock mass damage area, excavation damage area, blasting vibration damage accumulation, and other factors [29–32]. For instance, Chaboche [33] defined the concept of damage variables by using an indirect measurement program, then obtained different damage growth equations such as creep, ductile, and brittle damage. Using continuum mechanics and statistical fracture mechanics, Liu and Katsabanis [34] determined the minimum damage value under the crack density obtained by integrating the crack density function over time and then verified the feasibility and reliability of the model by field blasting test and numerical simulation. Concerning the evolutionary damage law of rock mass, Hao et al. [35] proposed an anisotropic damage model by analyzing the dynamic response of a granite site under blasting loads based on the theory of continuous damage mechanics. Other researchers also agree that the two main factors affecting rock mass damage are strain rate and rock dynamic fracture parameters. The damage of rock mass is mainly affected by explosive force, stress redistribution, and weathering. Ramulu et al. [36] discussed the influence of repeated blast loading on the damage of rock mass during tunnel blasting excavation and established an on-site damage model by using peak particle velocity and plastic deformation. Malmgren et al. [37] studied the damage distribution range in the construction process of mining and damage evolutionary characteristics of rock mass using digital imaging techniques. Ling et al. [38] constructed a multivariate discriminant analysis model for rock damage caused by blasting vibration. Liu et al. [39] studied the fracture process of rock mass by acoustic emission and microseismic monitoring under multihorizontal uniaxial load aimed at guiding the working time and working area of field personnel. The damage to blast-induced vibration can lead to the generation, expansion, and transfixion of microcracks or macrocracks during rock mass excavation by blasting, and in severe cases, it may result in spalling and collapse from the excavated surface [40–42]. In recent years, with the rapid development of computer technology, numerical simulation methods have been adopted to study the influence of blasting vibration on rock mass [43–49].

We can observe from the aforementioned references that significant efforts have been exerted to investigate rock damage according to the monitoring data obtained from field investigations. However, few studies have been conducted on the damage shape and size of shared rock in the neighborhood tunnel under cyclic blasting loads, and it lacks a principle to determine the sphere of influence of blasting. In the present study, the influences of surrounding rock at different levels and thickness of the shared rock on the lining structure of anterior excavating tunnel under blasting load of posterior excavating tunnel were analyzed by ultrasonic test. The engineering characteristics of the Liuyuetian neighborhood tunnel were considered. Furthermore, the spatiotemporal sphere of influence of cyclic blasting in shared rock as well as its variation law was characterized. The remainder of this paper is structured as follows. Section 2 introduces the principle of rock mass damage. Section 3 describes engineering background, test principles and equipment, and monitoring schemes. Then the ultrasonic test results of two typical sections are analyzed in Section 4, and the ultrasonic wave velocity distribution of shared rock in Section 5. Finally, the paper is concluded in Section 6.

2. Principle of Rock Mass Damage

Macroscopically, rock mass is considered as a continuous material with original defects in the damage mechanics theory; that is, rock mass is a continuum with many cracks [50–52]. The damage can be regarded as the opening and expansion of the original cracks due to the propagation, reflection, and interaction of the explosion stress wave, resulting in the deterioration of the rock mechanical properties such as elasticity modulus, wave velocity, damping, and frequency [53–55]. According to the change of elasticity modulus, Kawmaoto et al. [56] got the classic definition of damage variable D:

$$D = 1 - \frac{E}{E_0}, \tag{1}$$

where E_0 is the elasticity modulus of rock mass before blasting (MPa) and E is the equivalent elasticity modulus of rock mass after blasting (MPa).

According to the elastic wave theory, the elasticity moduli of rock mass before and after blasting are, respectively,

$$E_0 = \rho_0 v_0^2 \frac{(1-\mu_0)(1-2\mu_0)}{1+\mu_0}, \tag{2}$$

$$E = \rho v^2 \frac{(1-\mu)(1-2\mu)}{1+\mu}, \tag{3}$$

where ρ_0 and ρ are the densities of the bedrock before and after blasting, respectively; μ_0 and μ are Poisson's ratios of the bedrock before and after blasting, respectively; v_0 is the wave velocity of rock mass before blasting (m/s); and v is the wave velocity of rock mass corresponding to the same test position after blasting (m/s).

When the tunnel is excavated by smooth blasting or presplitting blasting, the property of the reserved surrounding rock will not change qualitatively before and after blasting.

Assuming that the density and Poisson's ratio of rock mass before and after blasting are approximately equal, that is, $\rho_0 = \rho$ and $\mu_0 = \mu$, then equations (1)~(3) give

$$D = 1 - \frac{E}{E_0} = 1 - \left(\frac{v}{v_0}\right)^2. \quad (4)$$

Therefore, the damage variable of rock mass can be approximately expressed by the changes of wave velocity of rock mass before and after blasting. In the field of blasting engineering, the allowable change rate of wave velocity before and after blasting can be determined according to the different damage control standards. For example, the change rate η of wave velocity before and after blasting is used to determine the damage degree of rock mass under the action of blasting load in the literature [57–59]:

$$\eta = \frac{v_0 - v}{v_0} = 1 - \frac{v}{v_0}. \quad (5)$$

When the change rate $\eta > 15\%$ before and after blasting, it can be judged that the rock mass is damaged. Therefore, the damage variable D can be expressed as

$$D = 1 - \frac{E}{E_0} = 1 - \left(\frac{v}{v_0}\right)^2 = 1 - (1 - \eta)^2. \quad (6)$$

At this moment, the damage threshold of rock mass is $D_{cr} = 0.28$. The damage threshold can be used to judge the sphere of influence of blasting to surrounding rock.

3. Engineering Background and Monitoring Schemes

3.1. Engineering Background. The Liuyuetian tunnel from Yongshun County to Jishou City is located in Yongshun, China. The entrance of the tunnel in Jishou City is connected to the Mengdonghe bridge. According to the standard of the International Tunnel Association, the Liuyuetian tunnel is a long tunnel with a length of 1010 m (ZK10 + 445–ZK11 + 455) on the left and 1015 m (YK10 + 440–YK11 + 455) on the right. The geography of this project is characterized by denudation and corrosion of low-mountain landscape. The natural slope of mountains in the portal section is 30° to 35°, accompanied with great topographic relief. According to highway tunnel design data, weak weathering limestone is the dominant rock in the tunnel range. The neighborhood tunnel is a structural form that connects a separated tunnel and a multiarch tunnel. Unlike the Sandwich wall of the multiarch tunnel, which is made of concrete, there is a reserved rock mass between the two holes of the neighborhood tunnel. The total length of the neighborhood tunnel is 77 m and the buried depth is 25 to 46 m. The clear spacing of shared rock is 3 to 6 m. The surrounding rock in the tunnel is mainly at level IV. The plan view of the neighborhood tunnel is shown in Figure 1, and the profile view of 1–1 is shown in Figure 2.

The Liuyuetian tunnel was designed and constructed based on the New Austrian tunneling method. The rock mass of the neighborhood tunnel was excavated by upper and lower benches to relieve any influence of blasting vibration on the remaining rock. Preliminary support is applied in a timely manner after completion of the excavation. The excavation of the upper bench adopts the blasting technique of wedge cut and the diameter of the blast hole is 42 mm. Smooth blasting was applied on periphery holes using #2 rock emulsion explosives. The blast holes are located at intervals of 50 cm.

3.2. Test Principle and Equipment. As an effective nondestructive method, ultrasonic testing has been widely used to detect and evaluate crack detection [60, 61], bolt looseness monitoring [62], corrosion detection [63], void detection [64, 65], rock mass damage [66], and others [67, 68]. The ultrasonic test aims to analyze the stress state and integrity of rock mass according to the propagation law of the ultrasonic wave velocity in rock mass. Influenced by structural surfaces with different mechanical properties, the ultrasonic wave may develop refraction, scattering, and thermal loss during propagation in rock mass, thereby resulting in geometric and physical attenuation. In practical engineering, different shapes and numbers of cracks and cavities exist in rock mass, which may affect the propagation velocity of the ultrasonic wave. When the distances of refraction, scattering, or diffraction of the ultrasonic wave are relatively long, the ultrasonic wave velocity declines greatly. Moreover, the velocities of the ultrasonic wave vary at different properties of rock masses. As the tunnel advances continuously, the stress equilibrium state of protolith is destroyed such that stresses in the rock mass are redistributed or form local stress concentration. The stress state and integrity of rock mass change greatly when frequent blasting loads are applied onto rock mass, thereby resulting in continuous reduction of the ultrasonic wave velocity.

In this test, single-hole ultrasonic test method is applied at the side wall of the tunnel, as shown in Figure 3. The monitoring apparatus is RSM-SY5 (T) nonmetallic ultrasonic wave apparatus that was made by the Institute of Rock and Soil Mechanics, Chinese Academy of Sciences, and consisted of a transmitting transducer and two receiving transducers. In ultrasonic testing, the one-transmitting-double-receiving probe is placed in the test hole, and water is used as a coupling agent. The entrance of hole is plugged with an air bag, and then the test hole is filled with water. The ultrasonic test site is presented in Figure 4.

3.3. On-Site Monitoring Schemes. According to the spatial layout of the neighborhood tunnel and mechanical properties of the rock mass, the shared rock on the side of the anterior excavating tunnel was selected as the monitoring position. Ultrasonic test holes were set in the level IV surrounding rock. Specifically, holes $L1$ and $L2$ were intended to monitor sections K11 + 390 and K11 + 395. Figure 5 shows the layout of the ultrasonic test hole.

The diameter of the ultrasonic test hole is 50 mm. Drilling depths of $L1$ and $L2$ are 5.4 m and 5.8 m, respectively. A 50 cm space is reserved between the bottom of the ultrasonic test hole and the side wall of the shared rock in the posterior excavating tunnel. All ultrasonic test holes tilt down by 5° with consideration of the coupling effect between the sensor and the hole wall. Fresh water is applied as the coupling agent in the test. The one-transmitting-double-receiving probe starts from the bottom to the entrance of the ultrasonic test hole at a sampling distance of 20 cm. This test

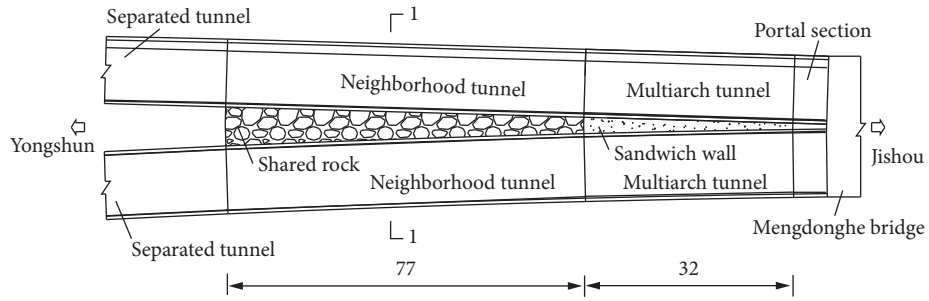

Figure 1: Plan view of the neighborhood tunnel (unit: m).

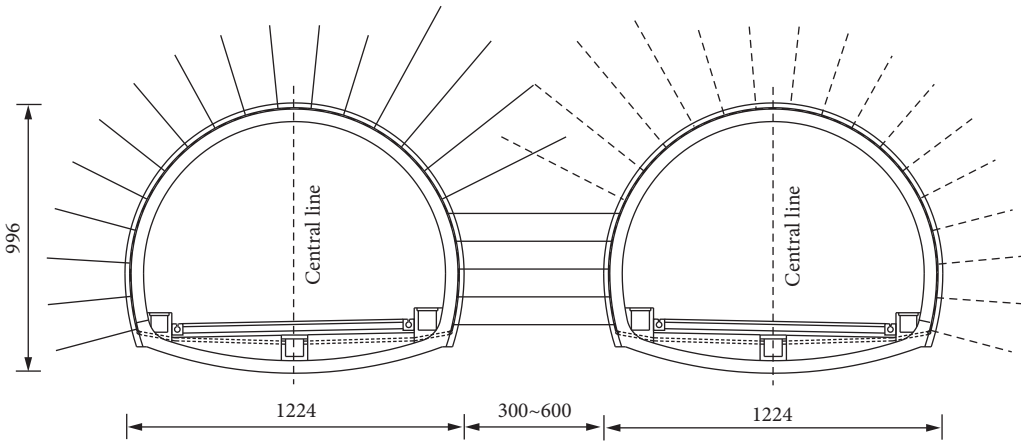

Figure 2: Profile view of 1–1 (unit: cm).

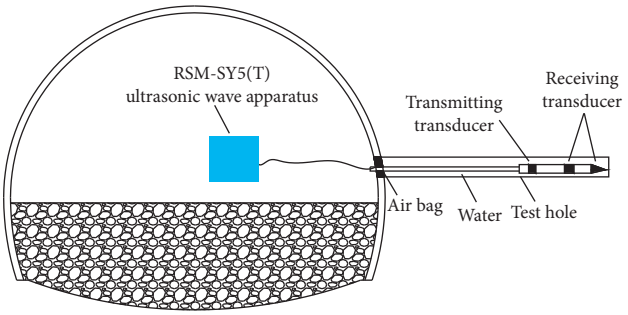

Figure 3: Schematic of single-hole ultrasonic test.

(a) (b)

Figure 4: (a) Test hole. (b) Ultrasonic wave apparatus in field test.

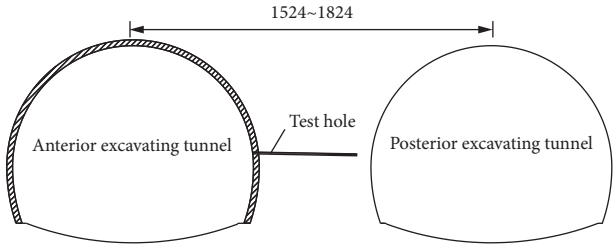

Figure 5: Profile of ultrasonic test hole (unit: cm).

mainly investigates damage on the shared rock within 5 to 6 m in the front and back of the test holes caused by blasting excavation. A total of six ultrasonic tests are conducted, including one ultrasonic test before the blasting and five ultrasonic tests after the blasting. The effects of the number of blasting on the ultrasonic wave velocity were analyzed according to the ultrasonic test results, thereby obtaining the variation law of ultrasonic wave velocity in the rock mass. Finally, the range and degree of damage accumulation were determined.

4. Ultrasonic Test Results Analysis

4.1. Ultrasonic Test Results of K11 + 390. Six tests of the ultrasonic wave velocity at $L1$ of the anterior excavating tunnel were conducted in the construction site. Five tests (K11 + 399, K11 + 396, K11 + 391, K11 + 388, and K11 + 383) were performed after blasting. The relation curves between the ultrasonic wave velocity and the hole depth at $L1$ on K11 + 390 are shown in Figure 6.

According to the test results in Figure 6, the ultrasonic wave velocity decreases continuously with the increase in the number of blasts, indicating that the damage to the surrounding rock is intensified continuously. When the hole depth is in the range of 1.4 to 3.4 m, the ultrasonic wave velocity at the test hole before blasting is higher than 4200 m/s, which agrees with the longitudinal wave velocity described by Ling et al. [38]. This condition reflects that the surrounding rock in this section is close to protolith and the integrity degree is relatively high, along with a low damage degree. However, the ultrasonic wave velocity drops dramatically by 42.6% from 5226 m/s at the hole depth of 1.4 m to 3050 m/s at 0.4 m. This condition proves that the integrity of the rock mass decreased and the load-bearing performance of the rock mass declines continuously. The ultrasonic wave velocity presents a monotone decreasing trend when the test hole is close to the anterior excavating tunnel, which is due to the blasting-induced damage to local shared rock. In the hole depth range of 3.4 to 5.8 m, the ultrasonic wave velocity in shared rock continues to decrease with the increase in the number of blasting in the posterior excavating tunnel. This condition demonstrates the occurrence of crack expansion in the shared rock in this section, which decreases the mechanical properties of rock mass significantly and forms a stress concentration zone.

To analyze the effects of the number of blasting on the damage accumulation degree of the shared rock, we formulate equation (1), which expresses the relationship between the hole depth and the damage variable. The relation curves are presented in Figure 7.

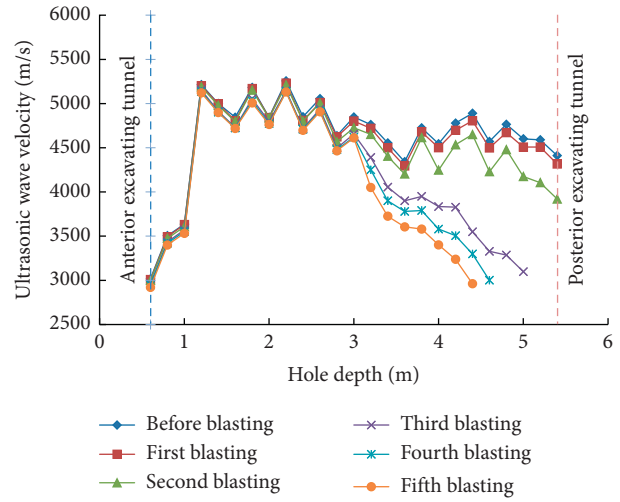

Figure 6: The relation curves between the ultrasonic wave velocity and the hole depth ($L1$).

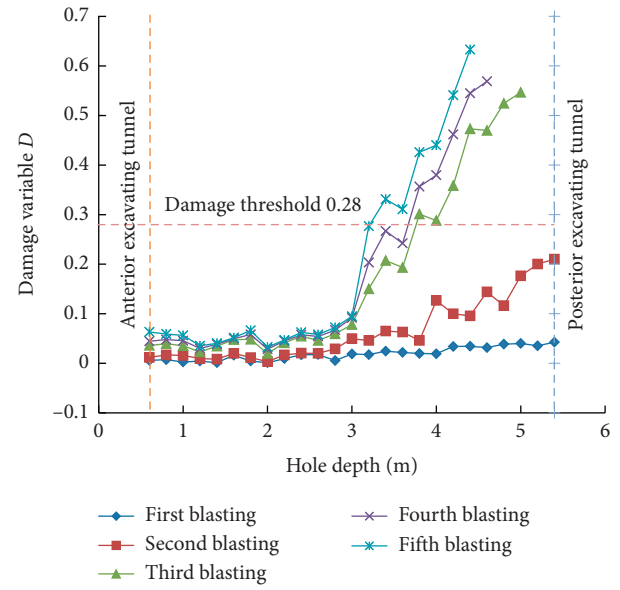

Figure 7: Relation curves between damage variable and hole depth ($L1$).

Figure 7 shows that, within the hole depth of 3.4 to 5.8 m, the mean D in five tests is 0.043, 0.044, 0.163, 0.051, and 0.045. Specifically, the D of the surrounding rock reaches the maximum (0.163) during the third blasting. According to damage judgment theory, the damage failure of rocks occurs when the D is higher than 0.28. In view of the relationship between D and hole depth, D is less than 0.28 in the first and second blasting excavations, indicating no damage to rocks. However, continuous blasting vibration still might cause deterioration to the physical and mechanical properties of the surrounding rock within a certain range, and cracks propagate continuously. The damage failure of rock mass initiates from the 4.6 m hole depth at the third blasting. According to the damage criterion of rock mass in Section 2, the damage range is determined at 2.2 m. The critical depth for rock failure at test holes is 4.2 m during the fourth blasting,

indicating that the damage range expands to a certain extent. The damage range remains the same at the fifth blasting, but the damage degree increases to a maximum of 0.61.

The relation curves between relative ultrasonic wave velocity in the shared rock and hole depth are shown in Figure 8. The relative ultrasonic wave velocity refers to the variation of the ultrasonic wave velocity in rock mass during one blasting compared with that in the previous blasting.

Figure 8 shows that the ultrasonic wave velocity attenuates slightly during the first blasting due to the long distance from the explosive source to the test hole. The relative ultrasonic wave velocity is controlled within 162 m/s. However, the relative ultrasonic wave velocity increases slightly during the second blasting, and the maximum value reaches 193 m/s. The relative ultrasonic wave velocity increases during the third blasting, reaching as high as 876 m/s. This result is related to the distance between the blasting hole and the surrounding rock at the test point. In addition, the damage degree of the surrounding rock increases quickly when the ultrasonic wave velocity attenuates significantly, and the region with high attenuation rates mainly concentrates in the depth range of 3.6 to 5.8 m. The boundary lines are obvious. The maximum relative ultrasonic wave velocities during the fourth and fifth blasting are 398 m/s and 415 m/s, respectively. The attenuation amplitudes are smaller than those in the third blasting. Given a similar distance between the explosive source and the test hole, the relative ultrasonic wave velocity in the fifth blasting is significantly higher than that in the first blasting. To sum up, the resistance of the shared rock to explosive loads drops dramatically with the increase in the number of blasting.

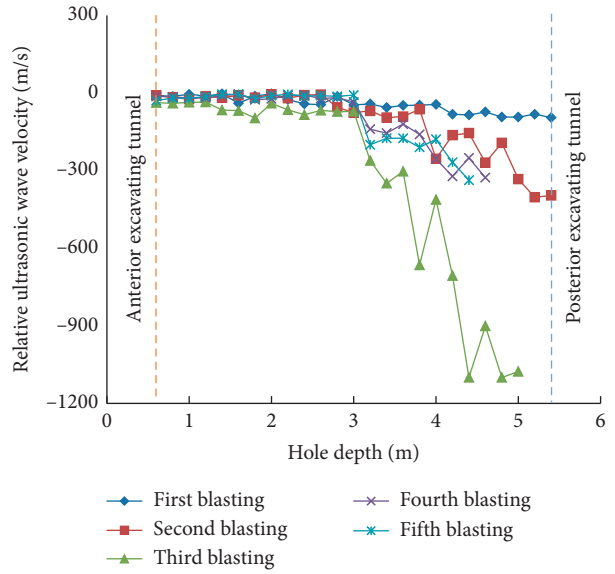

Figure 8: Relation curves between relative ultrasonic wave velocity and hole depth ($L1$).

4.2. Ultrasonic Test Results of K11 + 395. The ultrasonic wave velocity in one test before blasting and the ultrasonic wave velocity in five tests after blasting were collected from the anterior excavating tunnel section K11 + 395. Five blasting excavation faces of the posterior excavating tunnel existed, namely, K11 + 403, K11 + 399, K11 + 396, K11 + 391, and K11 + 388. The relation curves of ultrasonic wave velocity, damage variable, and relative ultrasonic wave velocity with hole depth are shown in Figures 9–11.

In Figure 9, the ultrasonic wave velocity within 1.2 to 5.4 m of the test hole before blasting is higher than 4300 m/s, which is consistent with the test results of $L1$. The ultrasonic wave velocity within 0.6 to 1.2 m drops significantly due to the damage of shared rock during the blasting excavation of the anterior excavating tunnel. The ultrasonic wave velocity decreases to different extents after multiple blasting of the posterior excavating tunnel. In particular, the ultrasonic wave velocity in the rock mass within 3.0 to 5.8 m of the hole depth decreases greatly at the third blasting, and the average reduction rate of the ultrasonic wave velocity reaches 13.4%.

Figure 10 shows that when the hole depth ranges from 3.0 to 5.4 m, the average damage variables of the ultrasonic wave velocity in five tests after blasting are 0.029, 0.082, 0.233, 0.066, and 0.063. Specifically, the damage variable of the surrounding rock reaches the maximum (0.233) during the third blasting, which is consistent with the ultrasonic wave velocity test results at $L1$. According to the damage

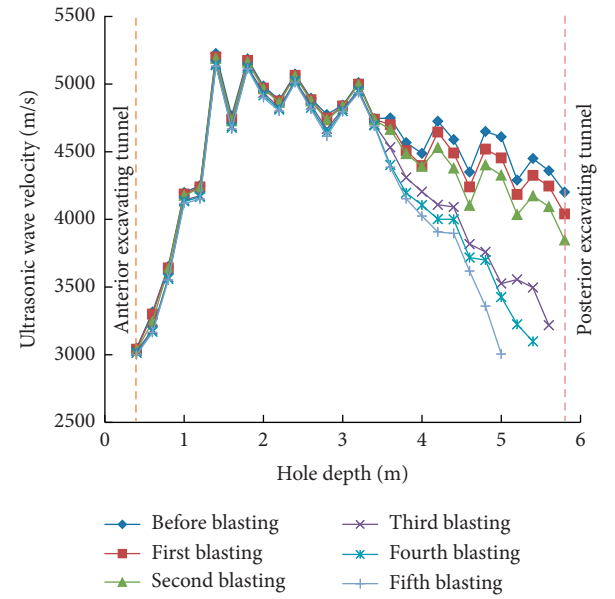

Figure 9: Relation curves between ultrasonic wave velocity and hole depth ($L2$).

criterion in Section 2, we can calculate that the damage accumulation range of the shared rock caused by the blasting of the posterior excavating tunnel is 2.4 m.

As shown in Figure 11, the maximum relative ultrasonic wave velocities in the five tests after blasting are 95, 403, 1100, 327, and 337 m/s. Similarly, the maximum relative ultrasonic wave velocity is also achieved in the third blasting. High values of the relative ultrasonic wave velocity mainly concentrate in the depth range of 3.0 to 5.4 m, indicating the serious damage of the surrounding rock in this section.

In other words, the attenuation laws of ultrasonic wave velocities at $L1$ and $L2$ are consistent. The damage range of shared rock under explosive loads is approximately 1.2 to

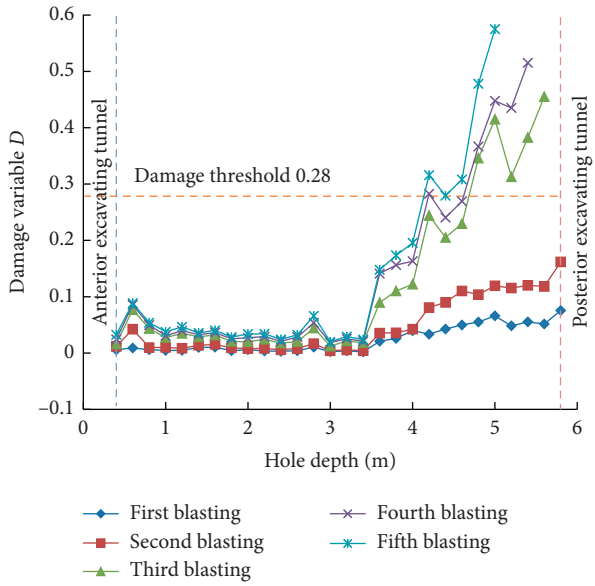

Figure 10: Relation curves between damage variable and hole depth ($L2$).

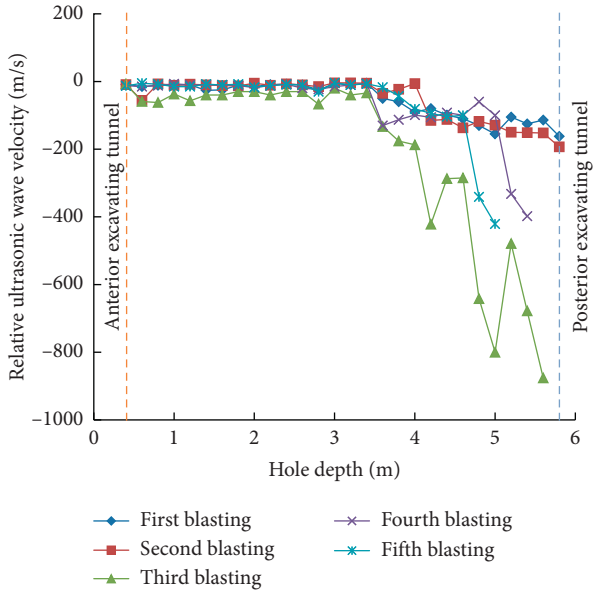

Figure 11: Relation curves between relative ultrasonic wave velocity and hole depth ($L2$).

1.4 m in the anterior excavating tunnel and approximately 2.2 to 2.4 m in the posterior excavating tunnel. The damage range of shared rock in the posterior excavating tunnel is 1.71 to 1.83 times that in the anterior excavating tunnel.

5. Distribution Law of Ultrasonic Wave Velocity of Shared Rock

5.1. Effects of Relative Ultrasonic Wave Velocity on Shared Rock. The region between $L1$ and $L2$ was set as the test region to analyze the effects of single blasting on the ultrasonic wave velocity (Figure 12). The variation laws of the

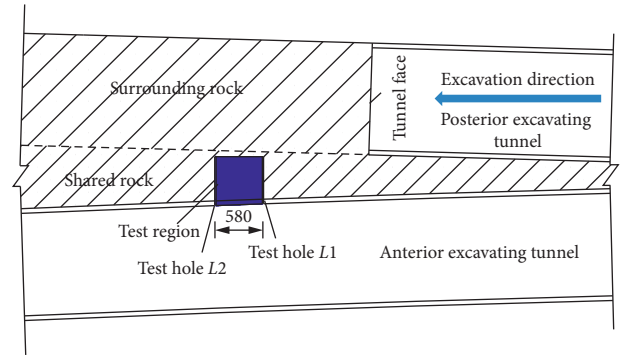

Figure 12: Layout of test region (unit: cm).

ultrasonic wave velocity in shared rock in the test region can be concluded by testing the ultrasonic wave velocity in blasting holes in the posterior excavating tunnel.

A widely accepted view is that cyclic blasting excavation may cause damage accumulation to shared rocks. Thus, the effects of each blasting on shared rock in the test region were analyzed by relative ultrasonic wave velocity. The posterior excavating tunnel had four blasting excavation faces, namely, K11 + 399, K11 + 396, K11 + 391, and K11 + 388. The variations of relative ultrasonic wave velocity in the test region under each blasting condition are presented in Figure 13. The monitoring section K11 + 395 is 0 m away from the vertical coordinate and K11 + 390 is 5 m away from the vertical coordinate.

Figure 13 shows that the relative ultrasonic wave velocity in shared rock in the test region changes greatly after each blasting. The excavation face during the first blasting is K11 + 399, and the maximum relative ultrasonic wave velocity difference is −492 m/s. The region with great attenuation amplitude of ultrasonic wave velocity is mainly in the area that is 0 to 2 m away from the side wall of the posterior excavating tunnel and has a hole depth of 5.0 to 5.4 m. The maximum relative ultrasonic wave velocity difference reaches −1220 m/s during the second blasting. The region with great attenuation amplitude is mainly located in the area that is 0–1.5 m away from the side wall of the posterior excavating tunnel and has a hole depth of 4 to 5 m. The reason is that this region is close to $L1$ and shows serious damage to the surrounding rock. The maximum relative ultrasonic wave velocity difference is −876 m/s during the third blasting. The region with great attenuation amplitude is mainly in the area that is 3 to 5 m away from the side wall of the posterior excavating tunnel and has a hole depth of 3.8 to 4.6 m. The excavation face is close to $L2$ during the third blasting, so the ultrasonic wave velocity at $L2$ attenuates quickly. The maximum relative ultrasonic wave velocity difference decreases to −398 m/s in the fourth blasting. The region with great attenuation amplitude is mainly located in the area that is 1 to 5 m away from the side wall of the posterior excavating tunnel and has a hole depth of 4.2 to 4.6 m.

Based on the preceding analysis, the maximum attenuation amplitude of the relative ultrasonic wave velocity is detected during the second blasting. The region with great attenuation amplitude is mainly located in the area that is 0 to 1.5 m and 4 to 5 m away from the side wall of the

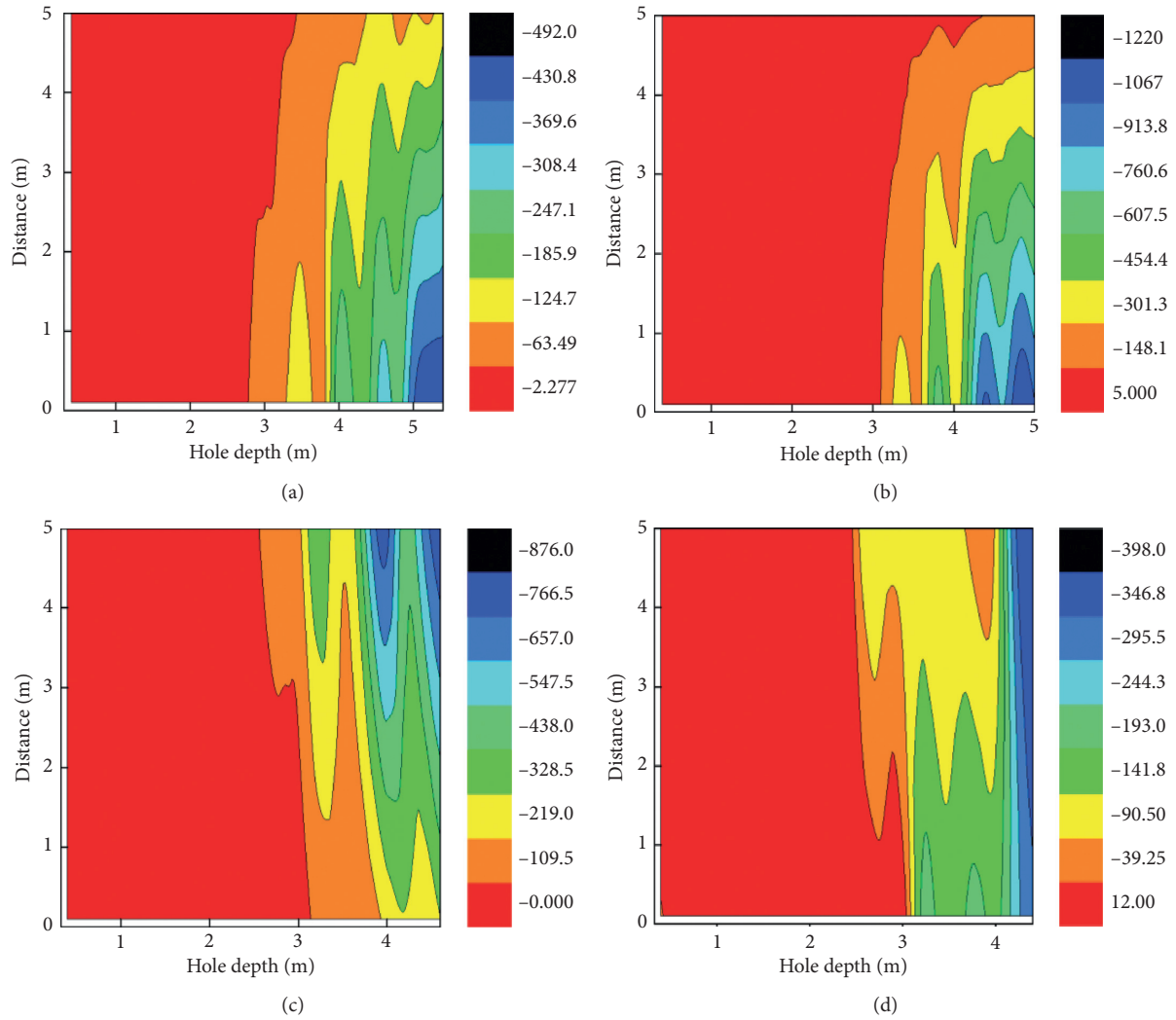

Figure 13: Nephograms of relative changes of ultrasonic wave velocity. (a) First blasting, (b) second blasting, (c) third blasting, and (d) fourth blasting (unit: m/s).

posterior excavating tunnel and has a hole depth of 3.8 to 5.0 m. Thus, stresses are relatively concentrated in local shared rock, thereby resulting in serious damage to the surrounding rock and significant attenuation of the ultrasonic wave velocity.

5.2. Effects of Absolute Ultrasonic Wave Velocity on Shared Rock. Figure 14 shows nephograms of the change process of the ultrasonic wave velocity in the test region after each blasting relative to the absolute ultrasonic wave velocity before blasting.

In ultrasonic wave velocity tests, the ultrasonic wave monitoring instrument cannot collect ultrasonic wave velocity due to serious damage to some shared rock, which decreases the hole depth after several numbers of blasting. Figure 14 shows the obvious attenuation region of the ultrasonic wave velocity of the rock mass. The attenuation rate is high when the hole depth is in the range of 3.5 to 5.4 m, and the absolute variation is higher than 1000 m/s. The maximum absolute variation (1355 m/s) of the ultrasonic wave velocity is in the region with 3.7 to 4.0 m depth and 3 to 5 m distance from the monitoring position.

Based on the preceding analysis, the stress concentration region of the shared rock is close to the excavation face under explosive loads of the posterior excavating tunnel. This region mainly distributes within 2 m along the longitudinal axis of the tunnel. This stress concentration region moves forward continuously as the excavation face advances. Finally, a strip stress concentration region that is approximately 2 m deep is formed.

In other words, determining the sphere of influence of cyclic explosive loads is important to support and protect the shared rock in the neighborhood tunnel. Crack expansion on surrounding rock stops after the dividing point is determined, accompanied by decelerating growth of the bulking force. The safe construction of the project can be ensured by strengthening supports to the surrounding rock and adjusting the sphere of influence of dynamic disturbances, including explosion.

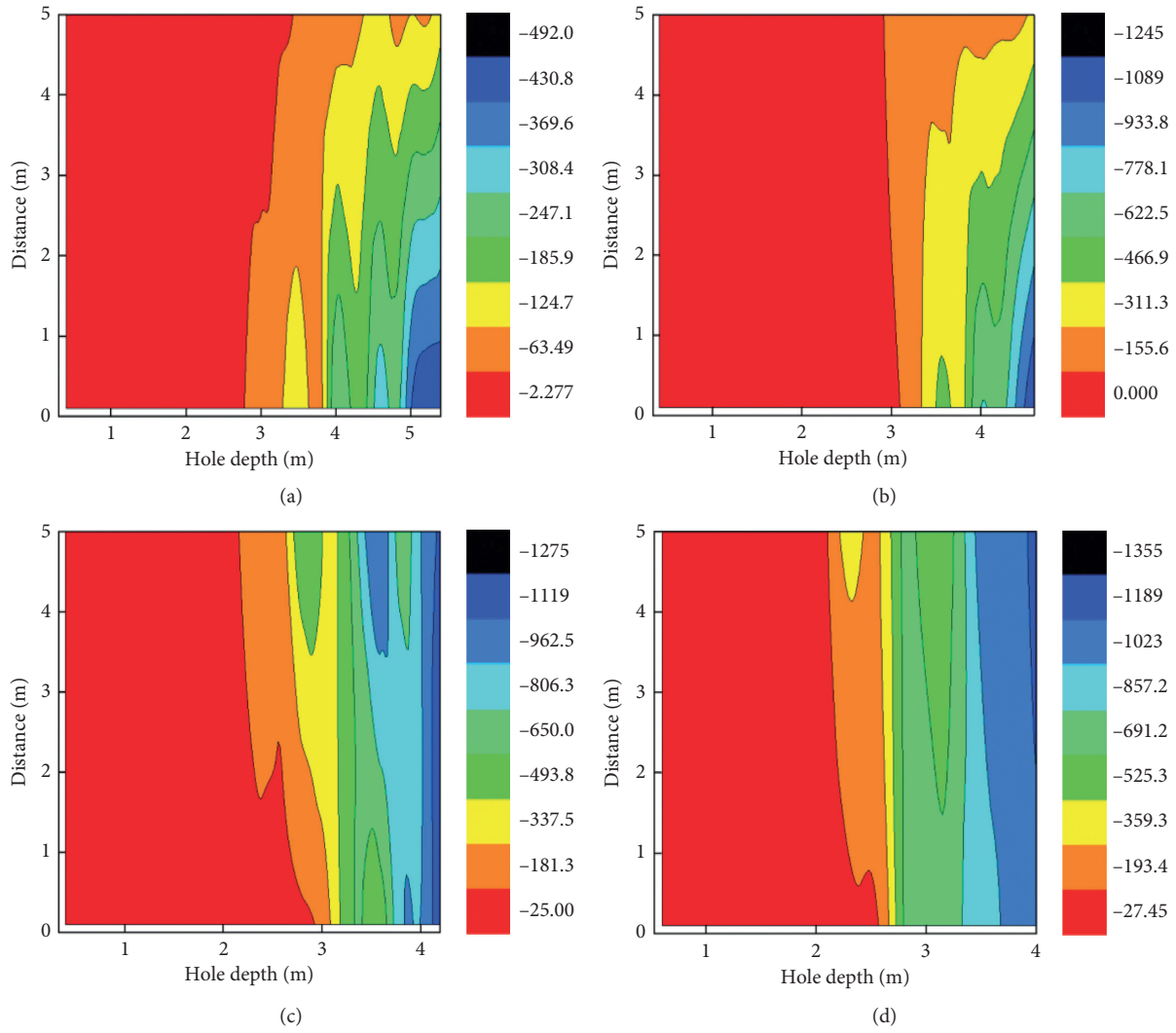

Figure 14: Nephograms of absolute changes of ultrasonic wave velocity. (a) First blasting, (b) second blasting, (c) third blasting, and (d) fourth blasting (unit: m/s).

6. Conclusions

The main objective of this study is to determine the damage range of the shared rock in the neighborhood tunnel during blasting excavation. Based on the field ultrasonic test presented in this study, the following conclusions can be drawn:

(1) Compared with single blasting, progressive cyclic explosions may cause damage accumulation to the shared rock in the neighborhood tunnel and the damage intensifies continuously. Therefore, the effects of damage accumulation have to be considered to evaluate the influences of explosive loads on the shared rock.

(2) During explosive excavation of the posterior excavating tunnel, the damage range of the shared rock is 1.2 to 1.4 m in the anterior excavating tunnel and 2.2 to 2.4 m in the posterior excavating tunnel. The damage range of the shared rock in the posterior excavating tunnel is approximately 1.71 to 1.83 times that in the anterior excavating tunnel.

(3) The stress concentration region of the shared rock is close to the excavation face under explosive loads of the posterior excavating tunnel and is mainly within 2 m along the longitudinal axis of the tunnel. The stress concentration region moves forward continuously as the excavation face advances. A strip stress concentration region that is approximately 2 m deep is formed gradually.

(4) A method to determine the sphere of influence of cyclic explosive loads on the shared rock is proposed. Variation law of the ultrasonic wave velocity in the shared rock under cyclic explosive loads is disclosed by analyzing the relative and absolute ultrasonic wave velocities.

Data Availability

All data used to support the findings of this study are included within the article. There are not any restrictions on data access.

Conflicts of Interest

The authors declare no conflicts of interest.

Acknowledgments

This work was supported by the National Natural Science Foundation of China (Nos. 51608183 and 51678071), the China Scholarship Council (No. 201808430341), and the Natural Science Foundation of Hunan Province in China (No. 2018JJ3022).

References

[1] N. Jiang, C. Zhou, X. Luo, and S. Lu, "Damage characteristics of surrounding rock subjected to VCR mining blasting shock," *Shock and Vibration*, vol. 2015, Article ID 373021, 8 pages, 2015.

[2] G. Liu, D. Song, Z. Chen, and J. Yang, "Dynamic response characteristics and failure mechanism of coal slopes with weak intercalated layers under blasting loads," *Advances in Civil Engineering*, vol. 2020, Article ID 5412795, 18 pages, 2020.

[3] A. Sharafat, W. A. Tanoli, G. Raptis, and J. W. Seo, "Controlled blasting in underground construction: a case study of a tunnel plug demolition in the Neelum Jhelum hydroelectric project," *Tunnelling and Underground Space Technology*, vol. 93, p. 103098, 2019.

[4] Z. Wang, C. Fang, Y. Chen, and W. Cheng, "A comparative study of delay time identification by vibration energy analysis in millisecond blasting," *International Journal of Rock Mechanics and Mining Sciences*, vol. 60, pp. 389–400, 2013.

[5] D.-X. Zhang, W.-Y. Guo, C.-W. Zang et al., "A new burst evaluation index of coal-rock combination specimen considering rebound and damage effects of rock," *Geomatics, Natural Hazards and Risk*, vol. 11, no. 1, pp. 984–999, 2020.

[6] X. Tian, Z. Song, and J. Wang, "Study on the propagation law of tunnel blasting vibration in stratum and blasting vibration reduction technology," *Soil Dynamics and Earthquake Engineering*, vol. 126, p. 105813, 2019.

[7] W.-b. Lu, Y. Luo, M. Chen, and D.-q. Shu, "An introduction to Chinese safety regulations for blasting vibration," *Environmental Earth Sciences*, vol. 67, no. 7, pp. 1951–1959, 2012.

[8] B.-y. Jiang, S.-t. Gu, L.-g. Wang, G.-c. Zhang, and W.-s. Li, "Strainburst process of marble in tunnel-excavation-induced stress path considering intermediate principal stress," *Journal of Central South University*, vol. 26, no. 4, pp. 984–999, 2019.

[9] J. Yang, J. Cai, C. Yao, P. Li, Q. Jiang, and C. Zhou, "Comparative study of tunnel blast-induced vibration on tunnel surfaces and inside surrounding rock," *Rock Mechanics and Rock Engineering*, vol. 52, no. 11, pp. 4747–4761, 2019.

[10] A. Li, D. Zhang, Q. Fang, J. Luo, L. Cao, and Z. Sun, "Safety distance of shotcrete subjected to blasting vibration in large-span high-speed railway tunnels," *Shock and Vibration*, vol. 2019, Article ID 2429713, 14 pages, 2019.

[11] S. Song, S. Li, L. Li et al., "Model test study on vibration blasting of large cross-section tunnel with small clearance in horizontal stratified surrounding rock," *Tunnelling and Underground Space Technology*, vol. 92, p. 103013, 2019.

[12] Y. Yao, C. He, and Z. Xie, "Study of mechanical behavior and reinforcing measures of middle rock wall of parallel tunnel with small interval," *Rock and Soil Mechanics*, vol. 28, pp. 1883–1888, 2007.

[13] H. Zhang, W. Qiu, and J. Feng, "Mechanical performance of shared rock of neighborhood tunnels," *Chinese Journal of Geotechnical Engineering*, vol. 32, pp. 434–439, 2010.

[14] Z. Zhong, Y. Tu, X. Liu, Y. Liu, and J. Zhang, "Calculation of lining loading of shallow-buried bilateral bias twin tunnel and its parameter sensitivity analysis," *China Civil Engineering Journal*, vol. 46, pp. 119–125, 2013.

[15] X.-Q. Fang, T.-F. Zhang, B.-L. Li, and R.-J. Yuan, "Elastic-slip interface effect on dynamic stress around twin tunnels in soil medium subjected to blast waves," *Computers and Geotechnics*, vol. 119, p. 103301, 2020.

[16] J. Chen, H. Yu, A. Bobet, and Y. Yuan, "Shaking table tests of transition tunnel connecting TBM and drill-and-blast tunnels," *Tunnelling and Underground Space Technology*, vol. 96, p. 103197, 2020.

[17] F. Cao, S. Zhang, and T. Ling, "Blasting-induced vibration response of the transition section in a branching-out tunnel and vibration control measures," *Advances in Civil Engineering*, vol. 2020, Article ID 6149452, 11 pages, 2020.

[18] B. Duan, W. Gong, G. Ta, X. Yang, and X. Zhang, "Influence of small, clear distance cross-tunnel blasting excavation on existing tunnel below," *Advances in Civil Engineering*, vol. 2019, Article ID 4970269, 16 pages, 2019.

[19] M. Yin, H. Jiang, Y. Jiang, Z. Sun, and Q. Wu, "Effect of the excavation clearance of an under-crossing shield tunnel on existing shield tunnels," *Tunnelling and Underground Space Technology*, vol. 78, pp. 245–258, 2018.

[20] N. Yugo and W. Shin, "Analysis of blasting damage in adjacent mining excavations," *Journal of Rock Mechanics and Geotechnical Engineering*, vol. 7, no. 3, pp. 282–290, 2015.

[21] C. Drover and E. Villaescusa, "A comparison of seismic response to conventional and face destress blasting during deep tunnel development," *Journal of Rock Mechanics and Geotechnical Engineering*, vol. 11, no. 5, pp. 965–978, 2019.

[22] C. Zang, M. Chen, G. Zhang, K. Wang, and D. Gu, "Research on the failure process and stability control technology in a deep roadway: numerical simulation and field test," *Energy Science & Engineering*, vol. 8, no. 7, pp. 2297–2310, 2020.

[23] J. H. Yang, Q. H. Jiang, Q. B. Zhang, and J. Zhao, "Dynamic stress adjustment and rock damage during blasting excavation in a deep-buried circular tunnel," *Tunnelling and Underground Space Technology*, vol. 71, pp. 591–604, 2018.

[24] L. Xie, P. Yan, W. Lu, M. Chen, and G. Wang, "Comparison of seismic effects during deep tunnel excavation with different methods," *Earthquake Engineering and Engineering Vibration*, vol. 17, no. 3, pp. 659–675, 2018.

[25] J. B. Martino and N. A. Chandler, "Excavation-induced damage studies at the underground research laboratory," *International Journal of Rock Mechanics and Mining Sciences*, vol. 41, no. 8, pp. 1413–1426, 2004.

[26] H. Li, X. Xia, J. Li, J. Zhao, B. Liu, and Y. Liu, "Rock damage control in bedrock blasting excavation for a nuclear power plant," *International Journal of Rock Mechanics and Mining Sciences*, vol. 48, pp. 210–218, 2011.

[27] G. R. Tripathy, R. R. Shirke, and M. D. Kudale, "Safety of engineered structures against blast vibrations: a case study," *Journal of Rock Mechanics and Geotechnical Engineering*, vol. 8, no. 2, pp. 248–255, 2016.

[28] F. He and G. Zhang, "Analysis and control of stability of the fractured soft rock surrounding a deep roadway," *Rock and Soil Mechanics*, vol. 36, pp. 1397–1406, 2015.

[29] H. K. Verma, N. K. Samadhiya, M. Singh, R. K. Goel, and P. K. Singh, "Blast induced rock mass damage around

tunnels," *Tunnelling and Underground Space Technology*, vol. 71, pp. 149–158, 2018.

[30] C.-P. Lu, L.-M. Dou, X.-R. Wu, and Y.-S. Xie, "Case study of blast-induced shock wave propagation in coal and rock," *International Journal of Rock Mechanics and Mining Sciences*, vol. 47, no. 6, pp. 1046–1054, 2010.

[31] F. Meng, C. Lin, L. Cai, and B. Li, "Cumulative damage evaluation of clip rock in small-distance tunnels caused by blasting excavation and its application," *Rock and Soil Mechanics*, vol. 32, pp. 1491–1499, 2011.

[32] M. Liu, G. Zhang, S. Liu, and Q. Li, "Research on accumulative damage effect of interlaid rock in Damaoshan tunnel group with small clear distance," *Chinese Journal of Rock Mechanics and Engineering*, vol. 28, pp. 1363–1369, 2009.

[33] J. L. Chaboche, "Continuum damage mechanics: part I-general concepts," *Journal of Applied Mechanics*, vol. 55, no. 1, pp. 59–64, 1988.

[34] L. Liu and P. D. Katsabanis, "Development of a continuum damage model for blasting analysis," *International Journal of Rock Mechanics and Mining Sciences*, vol. 34, no. 2, pp. 217–231, 1997.

[35] H. Hao, C. Wu, and Y. Zhou, "Numerical analysis of blast-induced stress waves in a rock mass with anisotropic continuum damage models part 1: equivalent material property approach," *Rock Mechanics and Rock Engineering*, vol. 35, no. 2, pp. 79–94, 2002.

[36] M. Ramulu, A. K. Chakraborty, and T. G. Sitharam, "Damage assessment of basaltic rock mass due to repeated blasting in a railway tunnelling project-a case study," *Tunnelling and Underground Space Technology*, vol. 24, no. 2, pp. 208–221, 2009.

[37] L. Malmgren, D. Saiang, J. Töyrä, and A. Bodare, "The excavation disturbed zone (EDZ) at Kiirunavaara mine, Sweden-by seismic measurements," *Journal of Applied Geophysics*, vol. 61, no. 1, pp. 1–15, 2007.

[38] T. Ling, Y. Liao, and S. Zhang, "Safety criterion method of rock blasting vibration damnification based on multivariant discriminant analysis model," *Journal of Central South University (Science and Technology)*, vol. 41, pp. 322–327, 2010.

[39] J. P. Liu, S. D. Xu, and Y. H. Li, "Analysis of rock mass stability according to power-law attenuation characteristics of acoustic emission and microseismic activities," *Tunnelling Underground Space Technol*, vol. 83, pp. 303–312, 2019.

[40] N. Jiang, T. Gao, C. Zhou, and X. Luo, "Effect of excavation blasting vibration on adjacent buried gas pipeline in a metro tunnel," *Tunnelling and Underground Space Technology*, vol. 81, pp. 590–601, 2018.

[41] W. Cheng, W. Wang, S. Huang, and P. Ma, "Acoustic emission monitoring of rockbursts during TBM-excavated headrace tunneling at Jinping II hydropower station," *Journal of Rock Mechanics and Geotechnical Engineering*, vol. 5, no. 6, pp. 486–494, 2013.

[42] J. Yang, W. Lu, M. Chen, P. Yan, and C. Zhou, "Microseism induced by transient release of in situ stress during deep rock mass excavation by blasting," *Rock Mechanics and Rock Engineering*, vol. 46, no. 4, pp. 859–875, 2012.

[43] H.-b. Zhao, Y. Long, X.-h. Li, and L. Lu, "Experimental and numerical investigation of the effect of blast-induced vibration from adjacent tunnel on existing tunnel," *KSCE Journal of Civil Engineering*, vol. 20, no. 1, pp. 431–439, 2016.

[44] X. F. Deng, J. B. Zhu, S. G. Chen, Z. Y. Zhao, Y. X. Zhou, and J. Zhao, "Numerical study on tunnel damage subject to blast-induced shock wave in jointed rock masses," *Tunnelling and Underground Space Technology*, vol. 43, pp. 88–100, 2014.

[45] A. Mahdiyar, D. Jahed Armaghani, M. Koopialipoor, A. Hedayat, A. Abdullah, and K. Yahya, "Practical risk assessment of ground vibrations resulting from blasting, using gene expression programming and Monte Carlo simulation techniques," *Applied Sciences*, vol. 10, no. 2, p. 472, 2020.

[46] Z. He, C. Li, Q. He, Y. Liu, and J. Chen, "Numerical parametric study of countermeasures to alleviate the tunnel excavation effects on an existing tunnel in a shallow-buried environment near a slope," *Applied Sciences*, vol. 10, no. 2, p. 608, 2020.

[47] X. Li, X. Zhou, B. Hong, and H. Zhu, "Experimental and numerical study on longitudinal axial force and deformation of shield tunnel," *Proceedings of GeoShanghai 2018 International Conference: Tunnelling and Underground Construction*, vol. 71, pp. 329–339, 2018.

[48] C. Li and X. Li, "Influence of wavelength-to-tunnel-diameter ratio on dynamic response of underground tunnels subjected to blasting loads," *International Journal of Rock Mechanics and Mining Sciences*, vol. 112, pp. 323–338, 2018.

[49] B. Jin, Y. Liu, C. Yang, Z. Tan, and J. Zhang, "Construction technique of long-span shallow-buried tunnel considering the optimal sequence of pilot-tunnel excavation," *Advances in Materials Science and Engineering*, vol. 2015, Article ID 491689, 8 pages, 2015.

[50] C.-b. Yan, "Blasting cumulative damage effects of underground engineering rock mass based on sonic wave measurement," *Journal of Central South University of Technology*, vol. 14, no. 2, pp. 230–235, 2007.

[51] A. Lisjak and G. Grasselli, "A review of discrete modeling techniques for fracturing processes in discontinuous rock masses," *Journal of Rock Mechanics and Geotechnical Engineering*, vol. 6, no. 4, pp. 301–314, 2014.

[52] H. Yoshida and H. Horii, "Micromechanics-based continuum model for a jointed rock mass and excavation analyses of a large-scale cavern," *International Journal of Rock Mechanics and Mining Sciences*, vol. 41, no. 1, pp. 119–145, 2004.

[53] X. Chai, S. Shi, Y. Yan, J. Li, and L. Zhang, "Key blasting parameters for deep-hole excavation in an underground tunnel of phosphorite mine," *Advances in Civil Engineering*, vol. 2019, Article ID 4924382, 9 pages, 2019.

[54] J. Wang, S. Tang, H. Zheng, C. Zhou, and M. Zhu, "Flexural behavior of a 30-meter full-scale simply supported prestressed concrete box girder," *Applied Sciences*, vol. 10, no. 9, p. 3076, 2020.

[55] S. Kepak, M. Stolarik, J. Nedoma, R. Martinek, J. Kolarik, and M. Pinka, "Alternative approaches to vibration measurement due to the blasting operation: a pilot study," *Sensors*, vol. 19, no. 19, p. 4084, 2019.

[56] T. Kawamoto, Y. Ichikawa, and T. Kyoya, "Deformation and fracturing behaviour of discontinuous rock mass and damage mechanics theory," *International Journal for Numerical and Analytical Methods in Geomechanics*, vol. 12, no. 1, pp. 1–30, 1988.

[57] Y. Wang, S. Wang, Y. Zhao, P. Guo, Y. Liu, and P. Cao, "Blast induced crack propagation and damage accumulation in rock mass containing initial damage," *Shock and Vibration*, vol. 2018, Article ID 3848620, 10 pages, 2018.

[58] DL/T5389-2007, *Construction Technical Specifications on Rock-Foundation Excavating Engineering of Hydraulic Structures*, China Electric Power Press, Beijing, China, 2007.

[59] Y. Zeng, H. Li, X. Xia, B. Liu, H. Zuo, and J. Jiang, "Blast-induced rock damage control in Fangchenggang nuclear power station, China," *Journal of Rock Mechanics and Geotechnical Engineering*, vol. 10, no. 5, pp. 914–923, 2018.

[60] N. Li, F. Wang, and G. Song, "New entropy-based vibro-acoustic modulation method for metal fatigue crack detection: an exploratory study," *Measurement*, vol. 150, p. 107075, 2020.
[61] W.-B. Lu, Y.-G. Hu, J.-H. Yang, M. Chen, and P. Yan, "Spatial distribution of excavation induced damage zone of high rock slope," *International Journal of Rock Mechanics and Mining Sciences*, vol. 64, pp. 181–191, 2013.
[62] N. Zhao, L. Huo, and G. Song, "A nonlinear ultrasonic method for real-time bolt looseness monitoring using PZT transducer-enabled vibro-acoustic modulation," *Journal of Intelligent Material Systems and Structures*, vol. 31, no. 3, pp. 364–376, 2019.
[63] M. Luo, W. Li, C. Hei, and G. Song, "Concrete infill monitoring in concrete-filled FRP tubes using a PZT-based ultrasonic time-of-flight method," *Sensors*, vol. 16, no. 12, p. 2083, 2016.
[64] S. Yan, B. Zhang, G. Song, and J. Lin, "PZT-based ultrasonic guided wave frequency dispersion characteristics of tubular structures for different interfacial boundaries," *Sensors*, vol. 18, no. 12, p. 4111, 2018.
[65] H.-x. Tang, S.-g. Long, and T. Li, "Quantitative evaluation of tunnel lining voids by acoustic spectrum analysis," *Construction and Building Materials*, vol. 228, p. 116762, 2019.
[66] T. Ling, F. Cao, S. Zhang, L. Zhang, and D. Gu, "Blast vibration characteristics of transition segment of a branch tunnel," *Journal of Vibration and Shock*, vol. 37, pp. 43–50, 2018.
[67] H. Azari, S. Nazarian, and D. Yuan, "Assessing sensitivity of impact echo and ultrasonic surface waves methods for nondestructive evaluation of concrete structures," *Construction and Building Materials*, vol. 71, pp. 384–391, 2014.
[68] H. Chu, X. Yang, S. Li, and W. Liang, "Experimental study on the blasting-vibration safety standard for young concrete based on the damage accumulation effect," *Construction and Building Materials*, vol. 217, pp. 20–27, 2019.